Chinese Journal of Chemical Engineering 27 (2019) 863–868

Contents lists available at ScienceDirect

Chinese Journal of Chemical Engineering

journal homepage: www.elsevier.com/locate/CJChE

Article

Adsorption/desorption of toluene on a hypercrosslinked polymeric resin in a highly humid gas stream

Bing Zhou [1], Bin Sun [1], Wenjuan Qiu [2], Ying Zhou [1,*], Junqian He [1], Xiao'ai Lu [1], Hanfeng Lu [1,*]

[1] Institute of Catalytic Reaction Engineering, College of Chemical Engineering, Zhejiang University of Technology, Hangzhou 310014, China
[2] College of Environment, Zhejiang University of Technology, Hangzhou 310014, China

ARTICLE INFO

Article history:
Received 23 May 2018
Received in revised form 26 September 2018
Accepted 28 September 2018
Available online 10 October 2018

Keywords:
Adsorption/desorption
volatile organic compounds (VOCs)
High humidity
Macromolecule resin

ABSTRACT

In many sources of volatile organic compounds (VOCs), large amounts of water vapor come from the air and the reactors. The relative humidity (RH) of exhaust gas is normally >60% and is supersaturated. Maintaining the property of adsorbent on VOCs in a highly humid gas stream is a serious industrial problem. In this study, the adsorption/desorption behavior of toluene in a micro-mesoporous polymeric resin was investigated in a highly humid environment to explore the influence of abound water vapor on resin adsorption and regeneration. This resin could selectively adsorb toluene at an RH of 80%, and its adsorption property was unaffected by the presence of water vapor. In the case of humidity saturation, the resin displayed a high adsorption capacity at a moisture content of <30%. Therefore, the polymer resin is an excellent water-resistant adsorbent of VOCs. In the regenerative experiment, the resin maintained its original adsorption capability after four adsorption/desorption cycles of toluene purging with nitrogen gas at 120 °C. The resin exhibited excellent regeneration performance at high humidity.

1. Introduction

Volatile organic compounds (VOCs) are among the most common atmospheric pollutants emitted by various industries, such as chemical, petroleum, medicine, paint, and printing industries [1–3]. These compounds can be removed and recovered from gas streams through adsorption, which is one of the most attractive and effective removal and recovery techniques [4,5]. The key component of adsorption is a porous solid adsorbent. For example, activated carbon and molecular sieve are applied extensively during the removal of VOCs from gas streams because of their high porosity and large surface area [6–9].

However, in many sources of VOCs, a large amount of water vapor comes from air and reactors. The relative humidity (RH) of exhaust gas is normally more than 60% and even supersaturated because of a large amount of condensed water existing in adsorption containers. The competitive adsorption of organic molecules and water molecules also affects the overall performance of adsorption [10]. Activated carbon materials are prepared through carbonization and activation. Activation is used for high-temperature treatment of water vapor in industries [11]. A large number of oxygenated groups are inevitably found on the surface of activated carbon, and they enhance the selective adsorption capacity of water molecules. As a result, the capability of activated carbon to adsorb organic molecules weakens at high humidity. Zeolite molecular sieves (ZSM-5 and USY) have a stable skeleton structure and a low Si/Al ratio and consequently exhibit strong moisture adsorption properties. Nevertheless, activated carbon and molecular sieve are unsuitable for application in high-humidity environments [12–14]. Therefore, efforts have been devoted to developing highly hydrophobic adsorbents for the separation and recovery of VOCs from industrial gases. Porous polymeric resin shows potential for adsorption because of its controllable pore structure and on site hydrophobicity and regenerability. Resin is also frequently used as an adsorbent in purification and separation [15–17].

This study aimed to explore the influence of abound water vapor on resin adsorption. Hydrophobic resin V-503 (poly (styrene-divinylbenzene) polymer, The Dow Chemical Company, USA) was used as an adsorbent to evaluate dynamic adsorption and desorption properties in humid environments. Toluene, which is a typical nonpolar and inert aromatic hydrocarbon, was used as a model adsorbate, and the regeneration performance of the resin was investigated through thermal nitrogen cyclic desorption. Our results could serve as a reference for future industrial applications of this resin.

* Corresponding authors at: Zhejiang University of Technology, 18 Chaowang Road, Hangzhou 310014, China.
E-mail addresses: wjfx@zjut.edu.cn (Y. Zhou), luhf@zjut.edu.cn (H. Lu).

https://doi.org/10.1016/j.cjche.2018.09.027
1004-9541/

2. Experimental

2.1. Materials and characterization

V-503 was dried at a reduced pressure and at 60 °C for 2 h to remove moisture and pore-forming agents. Toluene, which is a representative aromatic VOC, was applied during adsorption.

The pore texture of the polymeric adsorbent was examined through N_2 adsorption in an ASAP 2020 micropore analyzer isotherms at −196 °C. Specific surface area (S_{BET}) was calculated following Brunauer–Emmett–Teller method by using adsorption data acquired at a relative pressure (P/P_0) ranging from 0.05 to 0.25. The total pore volume was estimated on the basis of the amount adsorbed at a relative pressure of approximately 0.9929. Pore size distribution curves were derived from the analysis of the desorption branch of the isotherm following Barrett–Joyner–Halenda (BJH) algorithm. The thermal gravity (TG) and the derivative thermal gravity (DTG) of the samples were analyzed with a TG/DTG analyzer (NETZSCH, STA 409PC). The heating rate was set at 10 °C·min^{-1} from 20 °C to 400 °C under an N_2 flow of 50 ml·min^{-1}.

2.2. Adsorption performance test

2.2.1. Static adsorption of water vapor

In a static mode, the water vapor adsorption curve of the resin was obtained by adsorbing deionized water relative to the saturation vapor pressure at 40 °C, a saturated vapor pressure of steam of 7.38 kPa, and a mass concentration of 51.00 g·m^{-3}. The cubic reaction vessel made of a thin iron wire was placed in 0.5 g of the sample and then positioned at 5 mm above liquid level. This reactor was connected to the electronic balance, and quality was recorded every 2 min. The adsorption degree of water on the resin was reflected by the change in quality. Similarly, the static adsorption curves of water vapor and toluene on the resin were obtained by adsorbing deionized water and toluene respectively relative to the saturation vapor pressure at 30 °C and 50 °C.

2.2.2. Dynamic adsorption of VOCs

A dynamic adsorption system was composed of three components, namely, a gas distribution system, a detection system, and an adsorbent bed system [18]. In this system, gaseous toluene used as a model VOC was generated by bubbling liquid toluene at 0 °C with standard air flow, and the flow volume was regulated with a mass flow controller. The generated gaseous toluene was transferred to a buffer by air steam and diluted with air at the required concentration. The inlet toluene concentration was controlled at 5000 mg·m^{-3}, and the airspeed was maintained at 20000 ml·h^{-1}·g^{-1}. Hygrometric toluene gas (RH = 80%) was acquired by diluting air directly into deionized water at 30 °C. Gaseous toluene in a dry or hygrometric state was passed directly through a sample column at 30 °C. The column (8 mm in diameter) was packed with the adsorbent of approximately 0.5 g. The inlet and outlet toluene concentrations were monitored online by using a gas chromatograph (GC, 6890 N, Agilent Technologies Co., Ltd.) equipped with a flame ionization detector. Adsorption capacity was calculated in accordance with Eq. (1) as follows:

$$q = \frac{F \times C_0 \times 10^{-6}}{W}\left[t_s - \int_0^{t_s} \frac{C_i}{C_0} dt\right] \quad (1)$$

where q is the dynamic adsorption capacity (mg·g^{-1}); t_s is the time to reach adsorption equilibrium (min); F is the flow volume of carrier gas (air) (167 ml·min^{-1}); W is the mass of the adsorbent (g); C_0 is the inlet concentration of the adsorbed gas (mg·m^{-3}), and C_i is the outlet concentration of the adsorbed gas (mg·m^{-3}).

2.3. Desorption performance test

A desorption system comprised three components, namely, a temperature-controlled system, a gas detection system, and a desorption bed [19]. After toluene underwent saturated adsorption, the samples were regenerated by a hot N_2 stream of 20 ml·min^{-1}. At the beginning of desorption, N_2 was purged into the sample column, and the tube furnace was turned on to heat up to 120 °C at a heating rate of 5 °C·min^{-1}. The outlet toluene concentrations were monitored online through GC, and the entire desorption lasted 120 min. The samples were reused to measure the adsorption capability. The same procedure was repeated four times during the subsequent recycling.

3. Results and Discussion

3.1. Surface area and pore volume distribution

The N_2 adsorption, desorption isotherms, and pore size distribution at −196 °C of the polymer resin V-503 are demonstrated in Fig. 1. According to the International Union of Pure and Applied Chemistry classification, the adsorption isotherm of V-503 was close to type IV. In this case, the nitrogen adsorption isotherms showed three typical steps as the relative pressure increased. First, the N_2 adsorption amount of the sample reached a high level (>200 cm^3·g^{-1}) at a relative pressure of approximately 0.05, indicating that the adsorption curve exhibited a steep increase in the low-pressure region, which represented adsorption or condensation in small micropores. As the relative pressure increased (0.05–0.9), a type H4 hysteresis loop appeared, implying that V-503 was typically composed of microporous-mesoporous materials. Finally, the adsorbed amount increased quickly near the saturation pressure of nitrogen because of active capillary condensation, indicating the presence of some macropores in the resin. However, the adsorbed amount did not reach saturation until the relative pressure P/P_0 was at 1. This condition showed the multilayer adsorption phenomena on V-503. The pore size distribution curves based on the BJH method are shown in Fig. 1. The average pore size was 4.14 nm (Table 1). The surface area and pore volume based on N_2 adsorption and desorption curve at −196 °C are also listed in Table 1. The resin, which exhibited a relatively high specific surface area of 771 m^2·g^{-1} (with a microporous surface area accounting for 51%) and a large pore volume of 0.799 cm^3·g^{-1}, might present a sufficient adsorption potential [20,21].

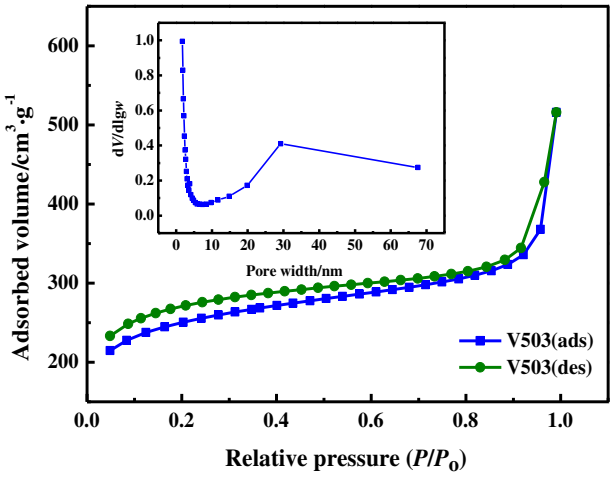

Fig. 1. N_2 adsorption–desorption isotherms and pore size distribution for resin.

Table 1
Structural characteristics of the resin

Sample	$S_{BET}/m^2 \cdot g^{-1}$	$S_{micro}/m^2 \cdot g^{-1}$	$S_{external}/m^2 \cdot g^{-1}$	$V_{pore}/cm^3 \cdot g^{-1}$	$V_{micro}/cm^3 \cdot g^{-1}$	$V_{external}/cm^3 \cdot g^{-1}$	D_{pore}/nm
V503	771	396	375	0.799	0.222	0.577	4.14

3.2. Static adsorption performance

Fig. 2 shows the static adsorption curve of dry resin under a hygrometric condition at 40 °C. The curves can be divided into three stages. During the first stage, the adsorption capacity increased rapidly because the adsorption position of the mesoporous pore was initially occupied by water vapor. When the adsorption time was from 50 min to 250 min, water vapor entered the microporous pore, and the adsorption capacity increased slowly. During the third stage, the adsorption reached equilibrium. V-503 obtained an adsorption amount of 126.13 $mg \cdot g^{-1}$. Consequently, the water content of V-503 was calculated as 11.20%, indicating the certain hygroscopic property of the polymer resin in humid environments. In addition, the surface of dry resin produced static electricity when particles rubbed against each other. Therefore, this type of polymer resin should be preserved under moist conditions.

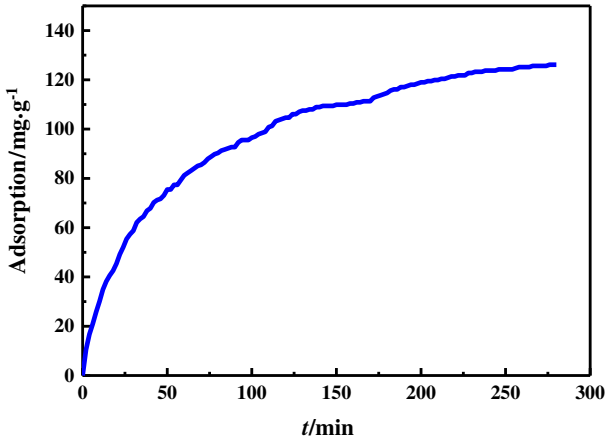

Fig. 2. Static adsorption curves of water vapor (RH = 100%) on the resin at 40 °C.

Fig. 3 presents the static adsorption curves of water vapor and toluene on the resin at 30 °C and 50 °C. The figure shows that the toluene adsorption capacity could reach 700 and 1200 $mg \cdot g^{-1}$ at 30 °C and 50 °C, respectively. V503 resin showed strong toluene adsorption.

3.3. Adsorption–desorption text under moist conditions

The influence of RH on breakthrough adsorption curves is shown in Fig. 4. The adsorption breakthrough time (126 min) and saturated adsorption capacity (210 $mg \cdot g^{-1}$) were calculated using the Y-N equation. The per square nanometer of the pores could adsorb two toluene molecules. The result demonstrated that a RH of 80% elicited a nearly negligible effect on the adsorption of toluene on polymeric adsorbents probably because toluene molecules are strongly adsorbed on the surface by replacing water molecules [15]. Thus, water weakly influenced toluene adsorption, and the effect of humidity on the adsorption of aromatic hydrocarbons by polymeric adsorbents could be disregarded in practical applications under these conditions.

Fig. 5 illustrates the obtained dynamic desorption curves of 20 $ml \cdot min^{-1}$ N_2 gas at 120 °C and the changes in the desorption rate. The outlet toluene concentration was monitored by GC at an interval of 5 min. The highest toluene concentration of 140000 $mg \cdot m^{-3}$ was

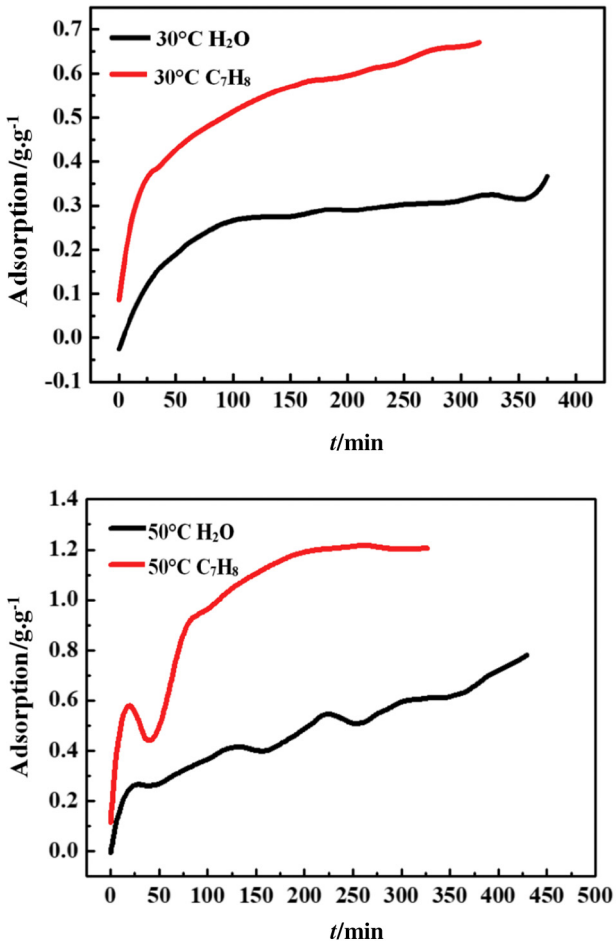

Fig. 3. Static adsorption curves of water vapor and toluene on the resin at 30 °C and 50 °C.

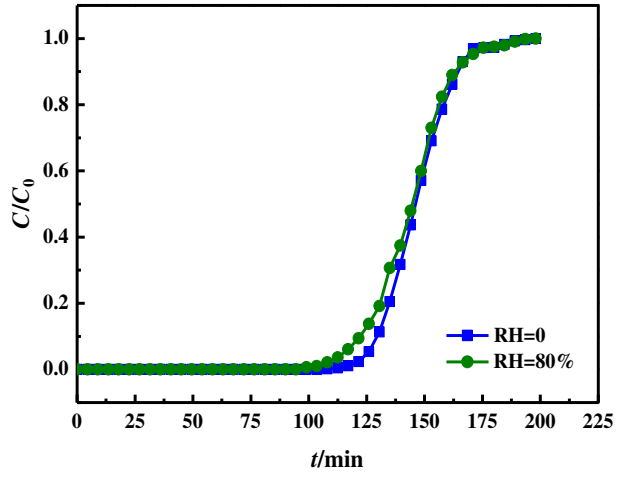

Fig. 4. Adsorbent curves of toluene on the resin at dry and wet air. [C: 5000 $mg \cdot m^{-3}$, GSHV: 20000 $ml \cdot h^{-1} \cdot g^{-1}$, T: 30 °C].

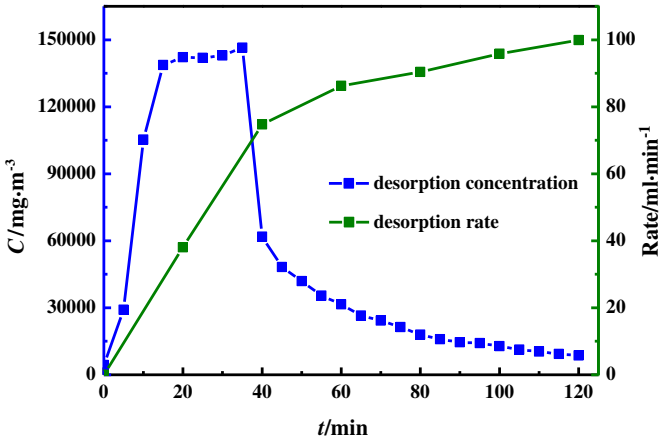

Fig. 5. Desorption concentration and rate curves of toluene on the resin at 120 °C with N_2 purging. (20 ml·min^{-1} N_2, 0~20 min: 20–120 °C, 20–120 min: 120 °C).

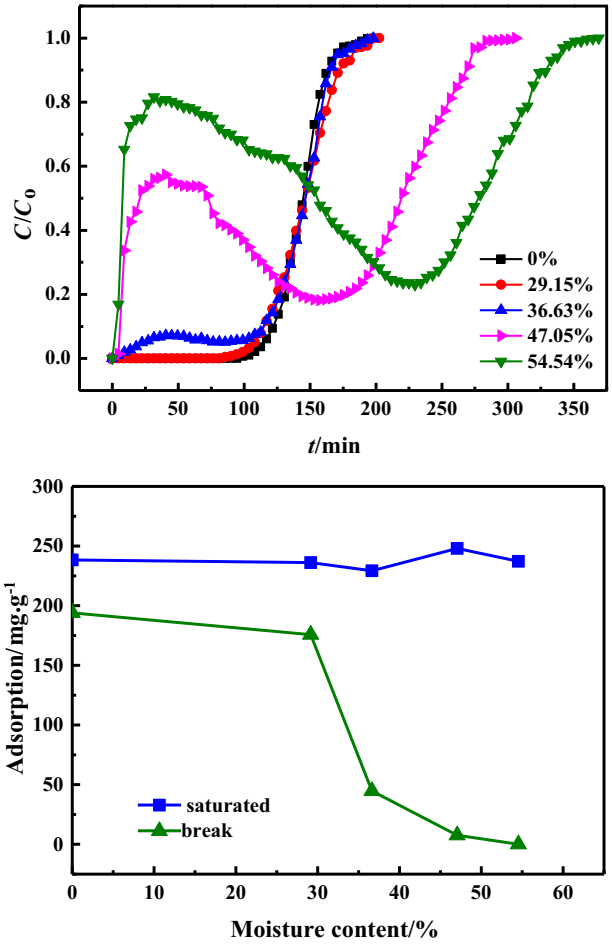

Fig. 6. Breakthrough curves and adsorption amounts of toluene on the resin at different water content. [C: 5000 mg·m^{-3}, GSHV: 20000 ml·h^{-1}·g^{-1}, *T*: 30 °C, RH = 80%].

observed after 20 min. This concentration exceeded the saturated vapor concentration of toluene at 0 °C. The result showed that the toluene molecules on the surface of the resin were removed rapidly as temperature increased. The adsorbent immediately maintained a supernal concentration of desorption for 20 min at a constant temperature. The desorption rate was approximately 80%. A high instantaneous desorption concentration corresponded to a high desorption rate. Although the concentration of toluene decreased quickly over time, the desorption rate reached 99% within 120 min. Thermal nitrogen purging could be applied to remove toluene on polymer resin.

In industries, adsorbents contain a large amount of water vapor similar to VOCs because of oversaturated water gas stream. Therefore, resins with different water contents should be prepared by soaking them in deionized water and then by purging with N_2 at a normal temperature to simulate the actual condition. In the current study, a dynamic adsorption experiment involving toluene (RH = 80%) on water-treated resin was conducted. The adsorption breakthrough curve was calculated (Fig. 6). The toluene concentration rapidly reached the breakthrough point, in which the outlet concentration was 5% of the inlet concentration, when the moisture content of the resin was more than 47.05%. The breakthrough curve became gentle because water molecules were replaced continually by toluene. The adsorption curve of the special resin with a moisture content of 36.63% was close to that of dry resin. The adsorption breakthrough time and saturated adsorption capacity are listed in Table 2. The resin still had a good adsorption capacity in spite of a slight decline from 238.3 mg·g^{-1} to 229.3 mg·g^{-1}. The quality of the system was also relatively balanced after adsorption. These results indicated that the initial water content slightly affected resin adsorption because it only retained the water content of the resin at less than 30% in the actual application.

3.4. Thermal stability text

The thermal stability of the resin was investigated by different aging times at specific temperatures. The aging time and temperature range should be determined. Fig. 7 presents the mass loss (TG) and differential

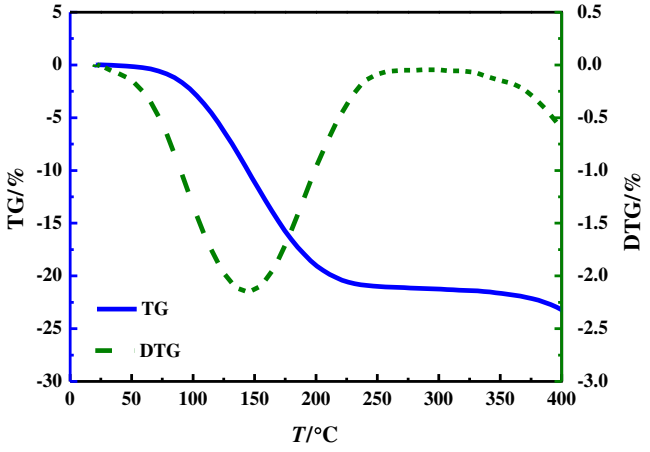

Fig. 7. TG, DTG curves of toluene on the resin.

Table 2
Adsorbent properties of toluene on the resin at different water content. (RH = 80%)

Moisture content/%	Saturated adsorption/mg·g^{-1}	Break through adsorption/mg·g^{-1}	Break through time/min	Water absorption capacity/mg·g^{-1}
0	238.3	194	117	15.6
29.15	236.1	175.7	108	14.4
36.63	229.3	44.7	27	15.3
47.05	248	7.6	4.5	13.6
54.54	237.2	0	0	15.4

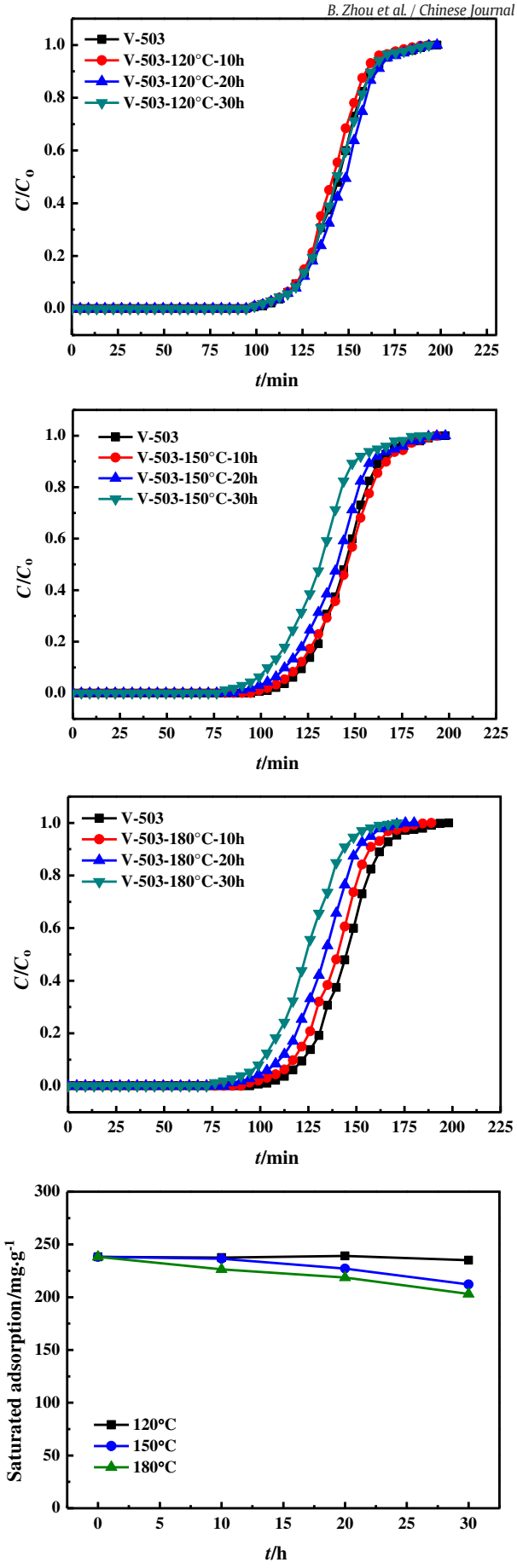

Fig. 8. Breakthrough curves and saturated adsorptions of toluene on resin after maturing. (C: 5000 mg·m^{-3}, GSHV: 20000 ml·h^{-1}·g^{-1}, *T*: 30 °C, RH = 80%).

mass analysis (DTG) of V-503. The TG curves of the sample revealed one stage of weight loss from 70 °C to 230 °C, with a thermodesorption peak centered at approximately 150 °C. Three temperatures (120 °C, 150 °C, and 180 °C) were used to examine the stability of the resin. Fig. 8 demonstrates the breakthrough curves of toluene on the resin aged at three temperatures. Toluene had no effect on adsorptive property after aging at 120 °C for a long time. However, the breakthrough time lagged at 150 °C for 30 h, and the saturation adsorption capacity decreased significantly from 238.3 mg·g^{-1} to 203.1 mg·g^{-1}. The collapsing of the porous structure of the macromolecule resin at a high temperature usually weakens the adsorptive property. The results showed that the observation was true for hot desorption at 120 °C. However, the thermal stability of polymer resin was relatively poor, and the resin must be used at less than 150 °C.

3.5. Regeneration capability

Thermal regeneration capability is one of the most important criteria for excellent VOC adsorption. After four adsorption and desorption cycles, toluene adsorption was slightly reduced after the desorption rate was maintained up to 95% (Fig. 9). The results clearly showed that the adsorbed toluene could be effectively removed under hot N_2 at 120 °C, indicating that the channel structure and surface properties of resin remain unchanged [22–24]. Therefore, the resin exhibited excellent regeneration performance at high humidities.

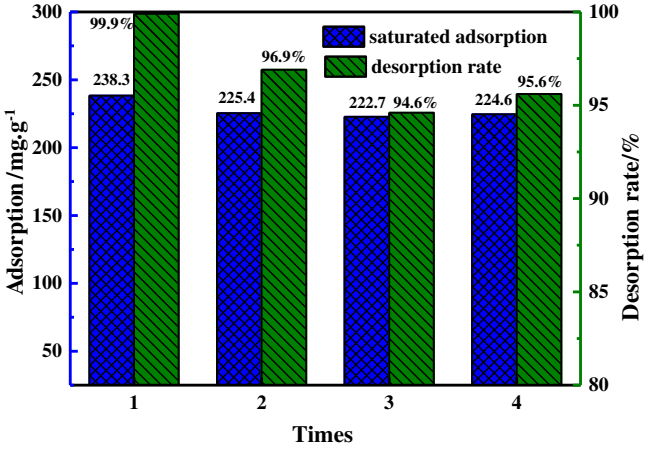

Fig. 9. Adsorbent/desorption properties of toluene on the resin after been cycle used for four times. [ads: C: 5000 mg·m^{-3}, GSHV: 20000 ml·h^{-1}·g^{-1}, *T*: 30 °C, RH = 80% des: 20 ml·min^{-1} N_2, 0–20 min: 20–120 °C, 20–120 min: 120 °C].

4. Conclusions

The adsorption property of toluene on the resin with a moisture content of less than 30% is consistent in high-humidity environments (RH = 80%) compared with that on dry resin. This result confirms that water vapor slightly influences the entire adsorption system. The macromolecule polymer resin presents high-adsorption capacity after four adsorption and desorption cycles, and the desorption rate is up to 95%. Therefore, the polymer resin can be a remarkable adsorbent for VOC removal in humid environments.

References

[1] G. Grażyna, C. Milena, W. Lidia, In vitro assays as a tool for determination of VOCs toxic effect on respiratory system: A critical review, *TrAC Trends Anal. Chem.* 77 (2016) 14–22.

[2] T. Petry, D. Vitale, F.J. Joachim, B. Smith, L. Cruse, R. Mascarenhas, S. Schneider, M. Singal, Human health risk evaluation of selected VOC, SVOC and particulate emissions from scented candles, *Regul. Toxicol. Pharmacol.* 69 (2014) 55–70.
[3] W. Wei, S.X. Wang, J.M. Hao, S. Cheng, Projection of anthropogenic volatile organic compounds (VOCs) emissions in China for the period 2010–2020, *J. Atmos. Environ.* 45 (2011) 6863–6871.
[4] R.R. Liu, C.D. Wu, M.J. Fu, Research review on volatile organic compounds (VOCs) removal by adsorption, *J. Guangdong Chem. Ind.* 41 (2014) 139–140.
[5] G. Rioland, H. Nouali, T.J. Daou, D. Faye, J. Patarin, Adsorption of volatile organic compounds in composite zeolites pellets for space decontamination, *Adsorption* 23 (2017) 395–403.
[6] K.J. Kim, C.S. Kang, Y.J. You, M.C. Chung, M.W. Woo, W.J. Jeong, N.C. Park, H.G. Ahn, Adsorption–desorption characteristics of VOCs over impregnated activated carbons, *Catal. Today* 111 (2006) 223–228.
[7] C.Y. Wu, T.W. Chung, T.C. Yang, M.T. Chen, Dynamic determination of the concentration of volatile alcohols in a fixed bed of zeolite 13X by FT-IR, *J. Hazard. Mater.* 137 (2006) 893–898.
[8] K.C. Nien, F.T. Chang, M.B. Chang, Adsorption-desorption characteristics of methyl ethyl ketone with modified activated carbon and inhibition of 2,3-butanediol production, *J. Air Waste Manage. Assoc.* 65 (2015) 1317–1326.
[9] F. Xin, Z.X. Yuan, W.C. Wang, Adsorption and desorption characteristics of allochroic silica gel and ZSM-5 zeolite to water, *Chem. Ind. Eng. Prog.* 34 (2015) 1730–1736.
[10] A. Iliyas, M.H. Zahedi-Niaki, M. Eić, S. Kaliaguine, Control of hydrocarbon cold-start emissions: a search for potential adsorbents, *Microporous Mesoporous Mater.* 102 (2007) 171–177.
[11] L.M. Sun, L.P. Zhang, J.H. Xue, B.Z. Li, Research Progress on preparation methods and applications of activated carbon, *Chem. Bioeng.* 33 (2016) 5–8.
[12] Q. Huang, X. Xue, R. Zhou, Catalytic behavior and durability of CeO_2, or/and CuO modified USY zeolite catalysts for decomposition of chlorinated volatile organic compounds, *J. Mol. Catal. A Chem.* 344 (2011) 74–82.
[13] Y.B. Liu, Y.Z. Li, X. Ding, Adsorption simulation of basic nitrogen compounds in ZSM-5 and USY zeolites by grand canonical Monte Carlo method, *Adv. Mater. Res.* 1096 (2015) 189–193.
[14] H. Zaitan, M.H. Manero, H. Valdés, Application of high silica zeolite ZSM-5 in a hybrid treatment process based on sequential adsorption and ozonation for VOCs elimination, *J. Environ. Sci.* 41 (2016) 59–68.
[15] L.J. Jia, W.H. Yu, C. Long, A.M. Li, Adsorption equilibrium and dynamics of gasoline vapors onto polymeric adsorbents, *Environ. Sci. Pollut. Res.* 21 (2014) 3756–3763.
[16] N. Fontanals, M. Galià, P.A.G. Cormack, R.M. Marcé, D.C. Sherrington, F. Borrull, Evaluation of a new hypercrosslinked polymer as a sorbent for solid-phase extraction of polar compounds, *J. Chromatogr. A* 1075 (2005) 51–56.
[17] C. Valderrama, J.L. Cortina, A. Farran, X. Gamisans, C. Lao, Kinetics of sorption of polyaromatic hydrocarbons onto granular activated carbon and Macronet hyper-cross-linked polymers (MN200), *J. Colloid Interface Sci.* 310 (2007) 35–46.
[18] H.F. Huang, X. Chu, H.F. Lu, B. Zhang, Y.F. Chen, Dynamic adsorption of volatile organic compounds on two kinds of mesoporous molecular sieves, *China Environ. Sci.* 30 (2010) 442–447.
[19] W.J. Qiu, K. Dou, Y. Zhou, H.F. Huang, Y.F. Chen, H.F. Lu, Hierarchical pore structure of activated carbon fabricated by CO_2/microwave for VOCs adsorption, *Chin. J. Chem. Eng.* 26 (2018) 81–88.
[20] H.F. Lu, J.J. Cao, Y. Zhou, D.L. Zhan, Y.F. Chen, Novel hydrophobic PDVB/R-SiO_2 for adsorption of volatile organic compounds from highly humid gas stream, *J. Hazard. Mater.* 262 (2013) 83–90.
[21] H.F. Huang, Y.Y. Gu, C. Yin, C.H. Zhou, H.F. Lu, The adsorption-desorption performance of volatile organic compounds(VOCs) onto polymer resin and mesoporous molecular sieves, *China Environ. Sci.* 32 (2012) 62–68.
[22] S.W. Nahm, G.S. Wang, Y.K. Park, C.K. Sang, Thermal and chemical regeneration of spent activated carbon and its adsorption property for toluene, *Chem. Eng. J.* 210 (2012) 500–509.
[23] W. Jiang, Study on Activated Carbon Fibers Adsorption-Nitrogen Desorption and Recover Multi-Component VOCs, Ms. Thesis, Huazhong University of Science and Technology, China, 2013.
[24] H.F. Huang, W.J. Rong, Y.Y. Gu, R.J. Chang, H.F. Lu, Adsorption and desorption of VOCs on the ZSM-5 zeolite, *Acta Sci. Circumst.* 34 (2014) 3144–3151.